Separation and Purification Technology 344 (2024) 127260

Contents lists available at ScienceDirect

Separation and Purification Technology

journal homepage: www.elsevier.com/locate/seppur

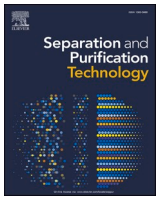

Biogas upgrading using shaped MOF MIL-160(Al) by pressure swing adsorption process: Experimental and dynamic modelling assessment

Mohsen Karimi [a,b,*], Rafael M. Siqueira [a,b], Alírio E. Rodrigues [a,b], Farid Nouar [c], José A. C. Silva [d,e], Christian Serre [c], Alexandre Ferreira [a,b]

[a] Laboratory of Separation and Reaction Engineering (LSRE), Associate Laboratory LSRE/LCM, Faculty of Engineering, University of Porto, Rua Dr. Roberto Frias, 4200-465 Porto, Portugal
[b] ALiCE - Associate Laboratory in Chemical Engineering, Faculty of Engineering, University of Porto, Rua Dr. Roberto Frias, 4200-465 Porto, Portugal
[c] Institut des Matériaux Poreux de Paris, ESPCI Paris, Ecole Normale Supérieure, CNRS, PSL University, Paris, France
[d] Centro de Investigação de Montanha (CIMO), Instituto Politécnico de Bragança, Campus de Santa Apolónia, 5300-253 Bragança, Portugal
[e] Laboratório Associado para a Sustentabilidade e Tecnologia em Regiões de Montanha (SusTEC), Instituto Politécnico de Bragança, Campus de Santa Apolónia, 5300-253 Bragança, Portugal

ARTICLE INFO

Editor: Z. Bao

Keywords:
Biogas upgrading
Adsorption
PSA process
MOF MIL-160(Al)
Sustainability

ABSTRACT

Biogas has been introduced as a sustainable source of energy, which is considered as a promising alternative for conventional fossil fuels. Indeed, biogas requires to be upgraded from the impurities, specifically, carbon dioxide to be commercially utilized. In this study, the potential of shaped form MIL-160(Al) as a water stable Al dicarboxylate microporous MOF has been assessed concerning the biogas upgrading application. To this end, firstly, the dynamic fixed-bed adsorption of carbon dioxide and methane was investigated at 313 K and 4.0 bar. The measured breakthrough outcomes were simulated with a developed mathematical model, which the results confirmed an acceptable potential of model predictions. Afterwards, a pressure swing adsorption (PSA) process with 5-steps was designed relying on dynamic equilibrium results, and experimentally validated by a lab-scale PSA set-up for a 50:50 CO_2/CH_4 mixture. Finally, an industrial PSA process was designed to have a precise knowledge on the potential of MIL-160(Al) for biogas upgrading for large scale applications. The results demonstrated the purity and recovery of methane around 99 % and 63 %, respectively, which indicated the appealing capacity of this adsorbent for such a purpose.

1. Introduction

Climate changes attributed to the global warming and exponential growth of energy consumption related to industrial development and population expansion are two of the major challenges of modern era [1–4]. Hence, the high energy demand has intensified the global fossil fuels consumption [5,6], which has severely impacted the environment through the global warming [7–9]. Accordingly, to reduce the fossil fuel consumption and also to provide the global required energy, the average annual renewable energy deployment showed a growth rate of 2.0 % since 1990 to 2018, which around 11.5 % of this growth related to the biogas [7,10,11], which Europe is considered as world leader of biomethane production [12]. The produced biogas can be directly utilized as a source of energy by introducing to the gas engines or gas turbines for electricity generation [13,14]. However, regarding the low efficiency of biogas to the electricity, which is around 10–16 %, the biogas upgrading and considering biomethane is preferred because of its higher energy density. Consequently, it can be employed as a clean energy in a broad range of applications including industrial plants or domestic usages [15,16].

Routinely, biogas is derived from the anaerobic digestion (AD) of organic matter, which based on the origin of the organic samples, it mostly includes CH_4 (35–70 %) and CO_2 (15–50 %), also minor quantities of H_2S (0–10,000 ppm), H_2O (0–10 %), NH_3, N_2, O_2, and CO, as well as volatile organic compounds can be traced in the biogas [12,17–19]. It is worth noting that currently different solid waste materials are considered as a source of biogas [20,21], which because of that, biogas can also be considered as a renewable source of energy [22]. A comparison between the typical compositions of biogas from different sources accompanied with related characteristics is presented in Table 1

* Corresponding author.
E-mail address: mohsen.karimi@fe.up.pt (M. Karimi).

https://doi.org/10.1016/j.seppur.2024.127260
Received 7 January 2024; Received in revised form 17 March 2024; Accepted 26 March 2024
Available online 27 March 2024

Table 1
A comparison between the typical compositions of biogas from different sources and related characteristics [7,23].

Parameters	*Biogas from Landfill*	*Anaerobic Digestion*	*Unit*
Methane	35–65	50–70	%
Carbon dioxide	15–50	30–50	%
Nitrogen	5–40	–	%
Oxygen	0–5	–	%
Hydrogen sulphide	0–100	0–10,000	ppm
Ammonia	5	<100	ppm
Total chlorine (as Cl^-)	20–200	0–5	mg/Nm^3
Lower Heating Value	12.3	20.2	MJ/kg
Density	1.3	1.2	kg/Nm^3
Wobbe index	18	27	MJ/Nm^3

Table 2
A summary of main characters of shaped form Al-based MOF MIL-160 [40].

Adsorbent Properties*	
Parameter	***Numerical Values***
Particle radius, (m)	0.001
Particle density at 0.0037 MPa, (g/mL)	1.07
Apparent (skeletal) density at 206.5 MPa, (g/mL)	1.40
Median pore diameter (volume) at 7.7 MPa and 0.1 mL/g, (μm)	0.162
Median pore diameter (area) at 119.8 MPa and 9.7 m^2/g, (μm)	0.0104
Average pore diameter (4 V/A), (μm)	0.0454
Total intrusion volume at 206.5 MPa, (mL/g)	0.22
Total pore area at 206.5 MPa, (m^2/g)	19.45
Micropore volume, (cm^3/g)	0.336

*Measured using Micrometric Instrument.

[7,23]. To meet the required standards and considered as a clean fuel, biogas must be purified by removing the impurities and upgraded by separating the carbon dioxide [17,24,25]. To date, different technologies have been evaluated for biogas upgrading including water scrubbing, physical scrubbing, chemical scrubbing, membrane, cryogenic and pressure swing adsorption [7,23], which detailed description of these technologies can be found in [23]. However, concerning the cost, energy consumption, efficiency and environmentally friendly, pressure swing adsorption using different classes of solid materials is among the most favorable ones [7,17,18].

1.1. Pressure swing adsorption (PSA)

After the emerge of cyclic adsorption processes [1], which was firstly

Table 3
Operating conditions and some specific properties of fixed-bed adsorption set-up.

Operating Conditions	***Numerical Values***
F (Flowrate), (Nml/min)	378.5
T (Temperature) (K)	313
P (Pressure) (bar)	4.1
CO_2/CH_4 composition	50/50
Ambient Temperature (K)	298
Adsorbent Properties	
Parameter	***Numerical Values***
Interparticle or bed porosity (m^3_{void}/m^3_{bed})	0.48
Intraparticle porosity (m^3_{void}/m^3_{bead})	0.31
Mass of sample (raw) (g)	12.2
Mass of sample (activated) (g)	10.9
Bed Characters	***Numerical Values***
Bed length, (cm)	6.8
Bed diameter, (cm)	2.1
Bulk bed density, (kg/m^3)	463.03

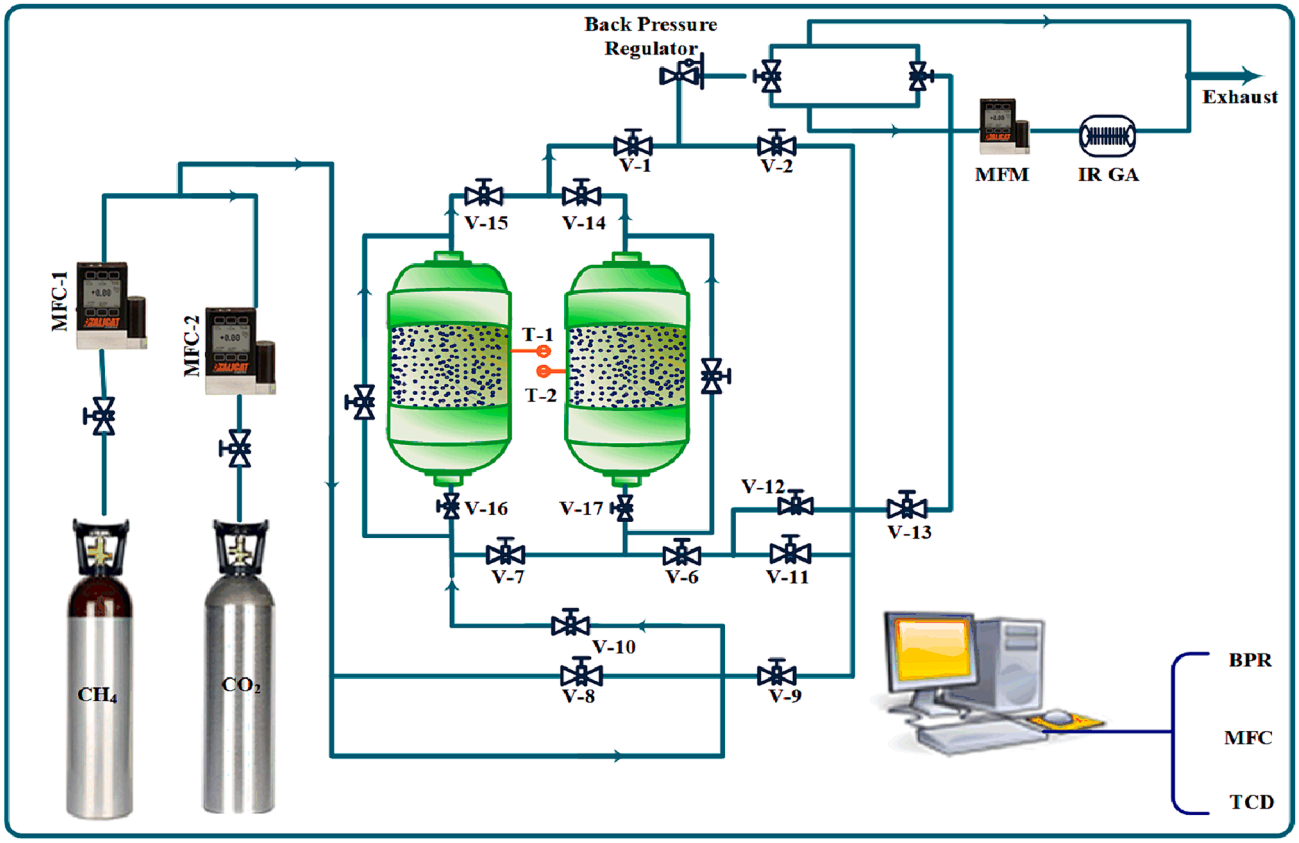

Fig. 1. A simple schematic of available lab-scale PSA set-up.

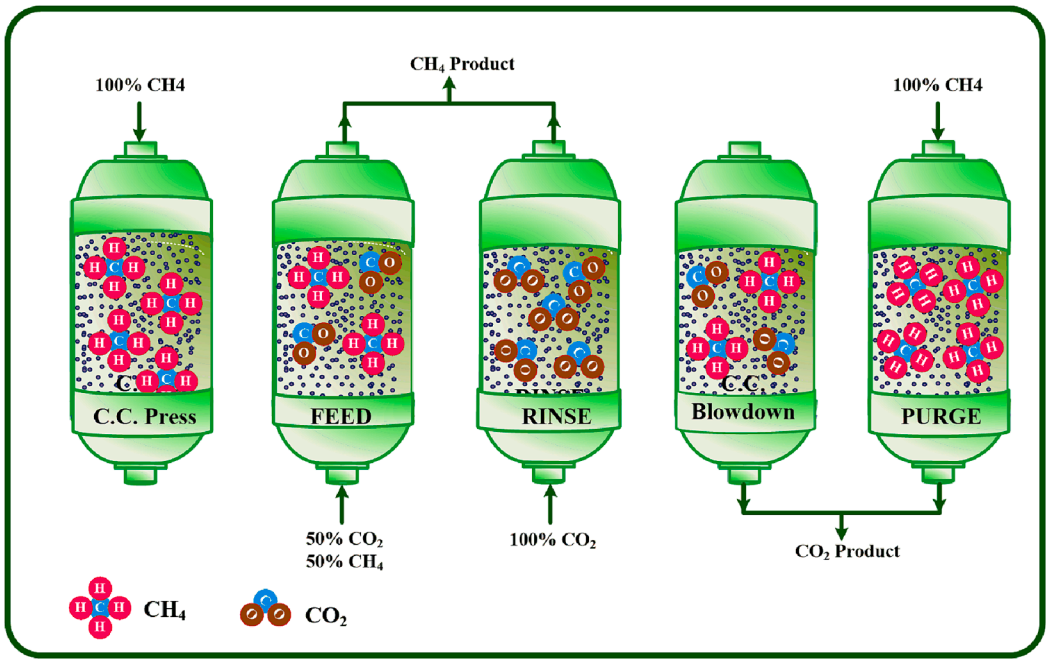

Fig. 2. Employed cycle sequences in the developed PSA experiments.

Table 4
A summary of key operating conditions of lab scale cyclic set-up.

PSA steps	*PSA variables Temperature (K)*	*Pressure (bar)*	*Flowrate (SLPM)*	*Step time (s)*	*CO_2%*	*CH_4%*
Pressurization	318	1 → 4.6	0.75	51	–	100
Feed	318	4.6	0.6	300	50	50
Rinse	318	4.6	0.3	350	100	0
Blowdown		4.6 → 1.0	–	50	–	–
Purge		1.0	0.1	60	–	100

patented by Skarstrom [26], PSA process has been a basic technology for gas separation because of its simplicity, acceptable energy yield, ability to control, and low capital/operating costs [17,27,28]. Designing a highly efficient PSA unit require a full set of engineering details and material characters. In this way, several operating factors including times and schedule of the various steps, flow rates, and pressure levels must be considered and optimized to develop an effective process [29,30]. On the other hand, the type of adsorbent is also one of the key elements in the adsorption process. Routinely, a proper adsorbent for separation processes should represent high selectivity, convenient loading capacity, service life and simplicity of regeneration [18,29]. To this end, in the last decades, a variety of microporous materials including activated carbons [31,32], zeolites [33–35], carbon molecular sieves [29], and metal–organic frameworks (MOFs) [36] have been tested for such a purpose.

1.2. Metal-organic frameworks (MOFs)

Lately, Metal-Organic Frameworks (MOFs) as a recent category of crystalline porous materials received a notable interest for gas adsorption processes [17,37] due to their exceptional diversity in terms of structural features, pore sizes/shapes and compositions. A summary of recent main studies on the developed MOFs for carbon capture and sequestration can be found in [38,39], associated with a wide domain of functionality for selectivity, thermodynamics and kinetics [40]. Accordingly, theses attractive characters nominated MOFs as favorable adsorbents for gas separation and purification studies. Despite mentioned benefits, still some main constraints limit the industrial-scale usage of this category of sorbents. For instance, the high synthesis cost is one of the main challenges for the large-scale application of these adsorbents, also the first proposed MOFs were poorly chemically stable or not thermally stable as well as most of them were available only in the powder from [37–39]. This is fortunately not anymore the case as many high valence based MOFs are hydrothermally stable [41], while their scale-up at the industrial scale is now becoming a reality [42]. Furthermore, in some cases, the high heat of adsorption limits their applications to be an ideal adsorbent for carbon capture and sequestration [17]. In this way, MIL-53(Al) already demonstrated an attractive potential for CO_2/CH_4 separation concerning the biogas upgrading [17]. Also, Abd et al. [43], investigated the UiO-66 for biogas upgrading to natural gas pipeline quality using pressure swing adsorption. They reported that the developed PSA upgrades the biogas with the purity of 98.2 % and recovery of 94.68 % [43]. On the other hand, concerning the viability of MOFs in presence of humidity and other impurities, Silva et al. [44], studied MIL-100(Fe) for atmospheric water harvesting by employing a cyclic adsorption process. It was found that MIL-100(Fe) remains stable during the water vapor contact and after exposure at different temperatures [44].

1.3. Research objective

Among numerous efforts made on developing MOFs [38,39], recently some of us developed the Al-based MOF denoted MIL-160 (MIL stands for Materials from Institut Lavoisier). This MOF, constructed from the bioderived FDCA feedstock (FDCA: Furane DiCarboxylic Acid), exhibits 1D microporous channels decorated with weak Bronsted acid sites

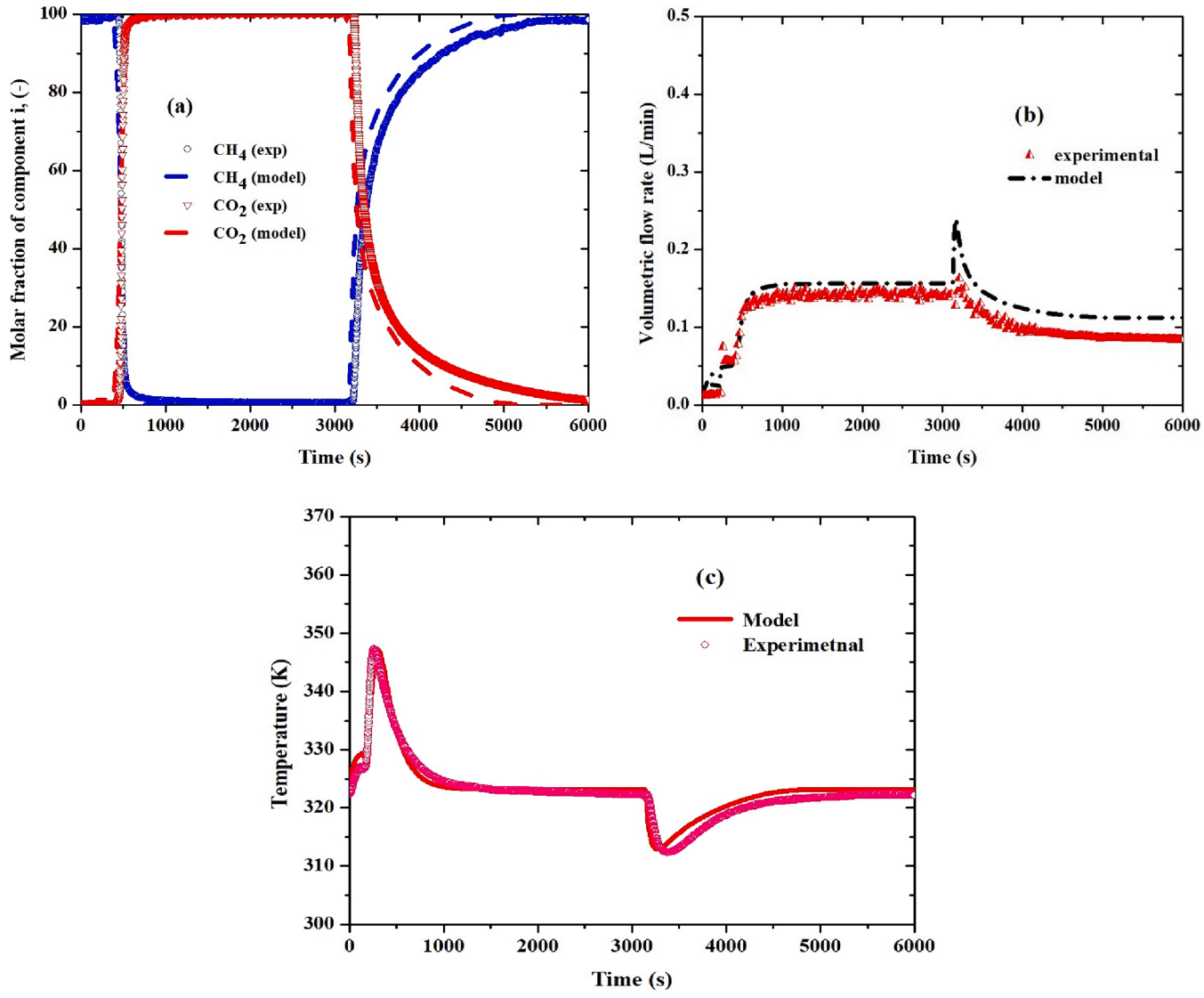

Fig. 3. Dynamic fixed-bed adsorption of carbon dioxide over the bed initially saturated with methane, the desorption with also pure methane, experiment at 313 K and 4.0 bar. (a) molar fraction, (b) flowrate and (c) temperature history. Symbols represents experimental results and lines indicates model outcomes.

Table 5
The considered parameters related to simulation of the breakthrough experiments.

$$q_i = q_{m1,i}\frac{b_{1,i}P_i}{1+b_{1,i}P_i} + q_{m2,i}\frac{b_{2,i}P_i}{1+b_{2,i}P_i}$$

$$b_i = b_{0,i} \times \exp\left(\frac{\Delta H_i}{RT}\right)$$

	CO_2	CH_4	unit
ΔH_1	21	12	kJ/mol
ΔH_2	3.5	5	kJ/mol
$b_{0,1}$	2.7×10^{-9}	6.6×10^{-9}	1/Pa
$b_{0,2}$	3×10^{-9}	1.9×10^{-7}	1/Pa
q_{m1}	5	5.2	mol/kg
q_{m2}	4.5	1.3	mol/kg

[45], while its excellent hydrothermal and thermal stability are of interest for many potential applications including heat reallocation. It can also easily be scaled-up under ambient pressure in water with a cheap cost production estimation at the industrial scale [36]. Once in shaped form (granules), it has already demonstrated promising specifications cornering the related heat pump/chiller applications [45–47] or the separation of branched alkanes under realistic conditions [48]. In addition, the study of loading capacity regarding the CO_2 and CH_4 adsorption, heat of adsorption, kinetic assessment, and selectivity showed its excellent capacity for biogas upgrading [40,49].

On these grounds, in the current study, the potential of MIL-160(Al) sample for separation of CO_2/CH_4 concerning the biogas application has been investigated using the PSA process for the first time. To this end, firstly, the dynamic of fixed-bed adsorption of carbon dioxide and menthane is accomplished, experimentally, and validated numerically. Afterwards, a 5-step PSA process is simulated and experimentally validated for biogas upgrading in a lab-scale set-up. Finally, a PSA process has been designed to evaluate the capacity of shaped MIL-160(Al) for biogas upgrading in the industrial scale.

2. Materials and methods

2.1. Materials and instrumentation

The synthesis protocol of MIL-160(Al) has already been described in [46]. However, here is a summary of main specifications. This adsorbent has a potential to be synthesized with a promising Space Time Yield (>160 $Kg.day^{-1}.m^{-3}$) by helicoidal *cis*-chains of $AlO_4(OH)_2$ octahedra connected through 2,5-FDCA ligands conducted to the microporous

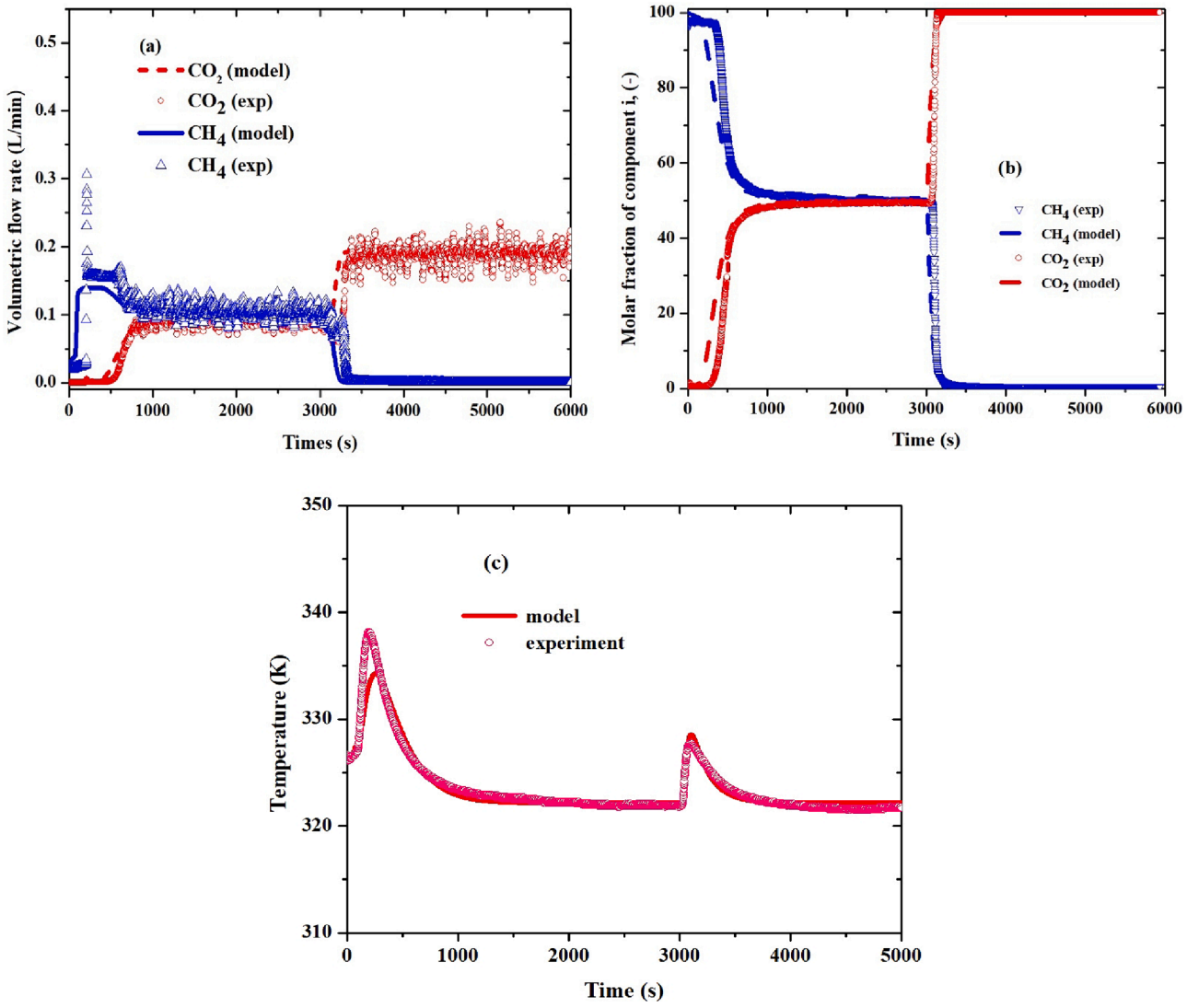

Fig. 4. Dynamic fixed-bed adsorption of pseudo binary CO_2(50 %)/CH_4(50 %) breakthrough experiment over the bed initially saturated with methane, the desorption/cleaning with pure carbon dioxide, experiment at 313 K and 4.0 bar. (a) partial flowrate (b) molar fraction and (c) temperature history. Symbols represents experimental results and lines indicates model outcomes.

channels of free aperture of 5–6 Å accompanied with isostructural from the parent CAU-10(Al) [45,46]. Regarding the microporous polar character of MIL-160(Al), it is highly proper for selective adsorption of polar molecules for pre-combustion processes including biogas upgrading while its moderate heat of adsorption enables a low temperature regeneration [45,46]. The shaping of the MOF was ensured by the wet granulation method, using a 5 wt% silica solution as the binder, leading to 1–2 mm size granules of a good mechanical stability and little decrease of pore volume compared to the bare powder. The main characterizations and textural properties of this adsorbent are reported in Table 2 [40], also N_2 adsorption–desorption isotherm at 77 K is also illustrated in Fig. S1 (Supporting Information). Further, carbon dioxide (99.99 %) and methane (99.95 %) as studied sorbates, as well as helium (99.999 %) as inert gas employed during the activation step were supplied by Air Liquide.

The dynamic breakthrough experiments and cyclic process were carried out by a fixed-bed dynamic set-up containing two columns, which to have the benefits of counter-current flows in the process, only one was employed in this study. Also, the feed flowrates were measured by mass flow controllers, while a mass flow meter was employed to monitor the flowrate at the outlet stream, all supplied by Alicat Scientific. In addition, the compositions of outlet gas from the adsorption column were continuously recorded using infrared gas analyzer. A thermocouple was improvised at the middle of column to record the temperature history during the adsorption process. Further, a back-pressure regulator was provided by Bronkhorst to control the pressure of system. A simple schema of this unit is illustrated in Fig. 1. Also, the main specifications of this experimental unit accompanied with operating conditions of breakthrough tests are described in Table 3.

2.2. Experimental procedures

In this work, the breakthrough tests and PSA cycles were developed in the same experimental set-up, which was already discussed. In this way, the activation procedure of virgin samples was accomplished by passing a helium flow with a flowrate of 378.5 Nml/min and heating up the bed with the rate of 1 K/min, up to 423 K, overnight. To perform the single component breakthrough test, the bed was firstly saturated with

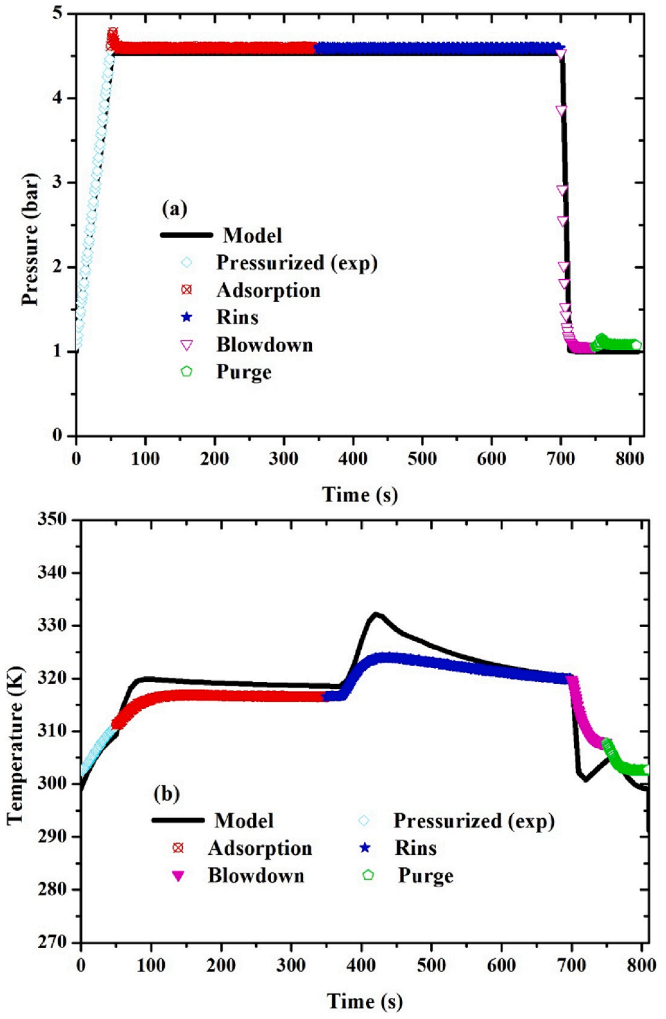

Fig. 5. The experimental and modeling outcomes of the cyclic steady state (cycle 12) of developed lab scale PSA process at 318 K and 4.6 bar. (a) pressure and (b) temperature history. Symbols represents experimental results and lines indicates model outcomes.

methane, afterwards, the feed (pure carbon dioxide) was infused to the system, which after getting the equilibrium conditions in the composition, pressure and temperature, the desorption step was accomplished by displacing the inlet stream to the CH_4. However, to fulfill the pseudo binary test, the bed was firstly saturated with CH_4, then, a stream containing CO_2 (50 %) / CH_4 (50 %) was fed to the adsorption column. It is noteworthy that in all adsorption–desorption experiments, the flowrate variations and temperature history were recorded, also an infrared gas analyser was employed to monitor the compositions at the outlet stream.

In the next phase, the PSA cycles containing five steps were designed and developed (represented in Fig. 2), at 318 K and 4.6 bar. To this end, the first cycle of PSA process initiated with pure methane in a counter-current way as the pressurization step, then the feed step was accomplished, afterwards, the rinse step performed using pure carbon dioxide, followed by blowdown and purge steps. It is worth noting, a pure flow of methane was counter-currently employed during the purge step to regenerate the bed. A summary of key operating conditions of developed PSA unit is reported in Table 4.

3. Mathematical model

Routinely, process design of adsorption technology requires robust mathematical approaches regarding the equilibrium values. Up to date, various models have been introduced to describe the adsorption isotherms, which Dual Site Langmuir (DSL) is among the most favorable ones because of its simplicity and accuracy for process simulation [50]. Accordingly, this model was employed to qualify the adsorption equilibrium values and developing the simulation of PSA cycles. This approach is described by Eq-1, where in this model, firstly, the strongest adsorption sites are filled followed by the weak adsorption energy sites [50,51], which after getting the equilibrium conditions in both sites, the constant values (b_1 and b_2) can be determined by Van't Hoff's equation (Eq-2) [50].

$$q_i = q_{m,1}\frac{b_1 P}{1+b_1 P} + q_{m,2}\frac{b_2 P}{1+b_2 P} \tag{1}$$

that q_i is the adsorbed concentration of the component i, q_m the saturation adsorbed concentration, P the equilibrium pressure, and b the adsorption affinity constant, presumed to change with temperature, according to the Van't-Hoff relation [50]:

$$b = b^{\infty}\exp\left(\frac{\Delta H}{RT}\right) \tag{2}$$

here, ΔH is the adsorption heat, R the ideal gas constant and b^{∞} is the adsorption affinity constant at infinite temperature.

Typically, to evaluate the dynamic paradigm of adsorption process, mathematical modeling is employed containing governor equations such as mass, energy and momentum balances accompanied with some auxiliary relations, which they have been discussed by details in Appendix A (Supporting Information). Further, here is some man assumptions considered during the development of the simulation procedure:

- The ideal gas law was considered for gas phase description.
- Mass transfer coefficients were assumed constants and described by lumped kinetic model.
- Energy pattern was characterized by non-isothermal and no-conduction model.
- Ergun equation was employed to describe the pressure drop in the system.
- Langer correlation was considered to describe the axial dispersion throughout the column [52].

In the next step, the simulation of PSA process was performed by employing proper boundary conditions, as reported in Table S1 (Supporting Information) coupled with developed dynamic fixed-bed adsorption model. Additionally, the yield of the PSA process can be assessed by product purity, recovery, and productivity factors as specified by Eqs. ((3)–(7)) [53].

$$CH_4 purity(\%) = \frac{\sum_j\left(\int_0^{t_j} F_{CH_4,out}dt\right)}{\sum_j\left(\int_0^{t_j} F_{CH_4,out}dt + \int_0^{t_j} F_{CO_2,out}dt\right)} \times 100 \tag{3}$$

$$CH_4 rec(\%) = \frac{\sum_j\left(\int_0^{t_j} F_{CH_4,out}dt\right) - \sum_k\left(\int_0^{t_k} F_{CH_4,in}dt\right)}{\sum_l\left(\int_0^{t_j} F_{CH_4,in}dt\right)} \times 100 \tag{4}$$

$$CO_2 purity(\%) = \frac{\sum_m\left(\int_0^{t_m} F_{CO_2,out}dt\right)}{\sum_m\left(\int_0^{t_m} F_{CH_4,out}dt + \int_0^{t_m} F_{CO_2,out}dt\right)} \times 100 \tag{5}$$

$$CO_2 rec(\%) = \frac{\sum_m\left(\int_0^{t_m} F_{CO_2,out}dt\right) - \sum_m\left(\int_0^{t} F_{CO_2,in}dt\right)}{\sum_l\left(\int_0^{t_l} F_{CO_2,in}dt\right)} \times 100 \tag{6}$$

$$CH_4 productivity\left(molkg^{-1}h^{-1}\right) = \frac{\sum_j\left(\int_0^{t_j} F_{CH_4,out}dt\right) - \sum_k\left(\int_0^{t_k} F_{CH_4,in}dt\right)}{massofdryadsorbent \times t_{cycle}} \tag{7}$$

Here, l is the feed, counter-current pressurization, j is the feed, rinse, k is the purge, counter-current pressurization, and m is the blowdown,

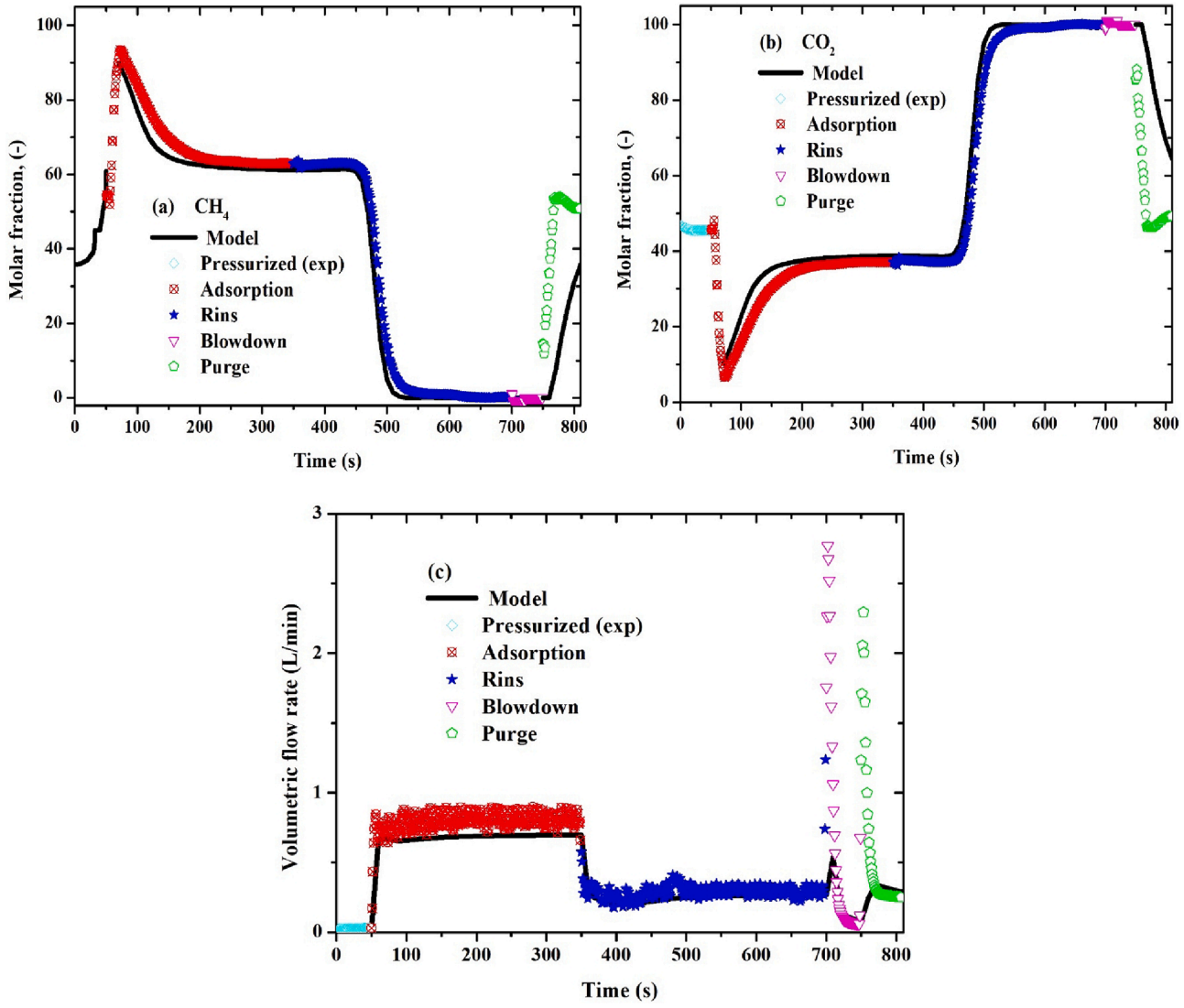

Fig. 6. Fig. The experimental and modeling outcomes of the cyclic steady state (cycle 12) of developed lab scale PSA process at 318 K and 4.6 bar. (a) methane molar fraction (b) carbon dioxide molar fraction, and (c) total volumetric flowrate. Symbols represents experimental results and lines indicates model outcomes.

Table 6
The characteristics of designed industrial PSA process for biogas upgrading.

	Unit	Value
Bulk bed density	$kg.m^{-3}$	548.90
Particle radius	m	1.35×10^{-3}
Bed porosity	–	0.487
Bed volume	m^3	10.61
Bed area	m^2	1.77

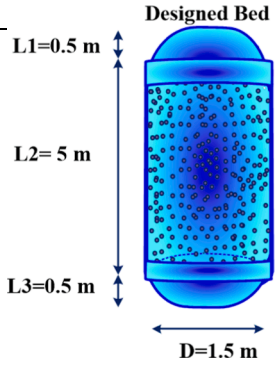

Table 7
The specifications of designed industrial PSA process accompanied with obtained purity, recovery and productivity of methane and carbon dioxide.

PSA steps	PSA variables					
	Temperature (K)	Pressure (bar)	Flowrate (SLPM)	Step time (s)	CO_2%	CH_4%
Pressurization	318	1 → 4.0	35,000	230	–	100
Feed	318	4.0	100,000	170	40	60
Rinse	318	4.0	45,000	100	100	0
Blowdown		4.0 → 1.0	0	75	–	–
Purge		1.0 → 0.2	8000	340	–	100
Performance of designed industrial PSA						
	Purity (%)		***Recovery (%)***		***Productivity (mol $kg^{-1}h^{-1}$)***	
CH_4	99.5		66.0		14.09	
CO_2	76.1		97.0		6.54	

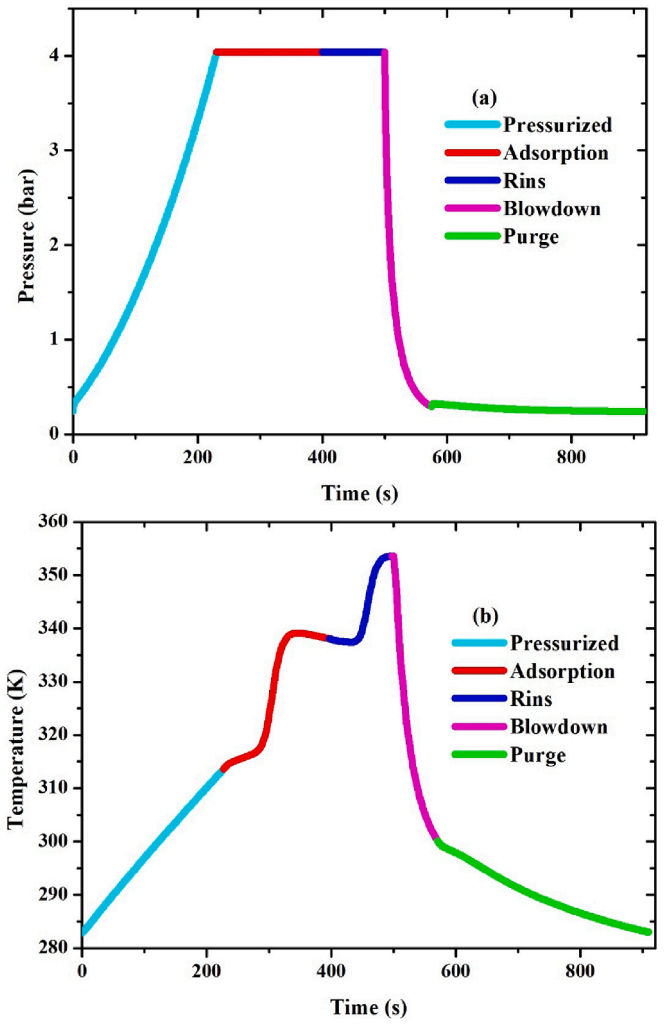

Fig. 7. The outcomes of developed industrial PSA process at the end of each step of the cyclic steady state (CSS), at 318 K and 4.0 bar. (a) pressure and (b) temperature history.

purge. It is worth noting that the developed model for dynamic simulation was solved by the gPROMS platform using a second order orthogonal collocation over twenty-eight finite elements.

4. Results and discussion

4.1. Breakthrough experiments and simulation

Fig. 3 illustrates breakthrough experiment ((3a) molar fraction, (3b) flowrate and (3c) temperature history) of CH_4-CO_2 onto shaped MIL-160 (Al) particles accompanied with prediction/simulation results as well as the temperature history. Also, the considered parameters related to the simulation of the breakthrough experiments have been presented in Table 5. As can be observed in Fig. 3a, the column is firstly fully saturated with CH_4 (for 400 s), afterwards, the pure flow of CO_2 is fed to the bed, which it takes around 225 s, to completely displaced with adsorbed methane. Further, the fast increase in the flowrate (Fig. 3b) corresponds to CH_4 that is fed accompanied with displaced adsorbed carbon dioxide. During the adsorption–desorption processes, in the second step, CO_2 is adsorbed as long as CH_4 is desorbed. Regarding the temperature history (Fig. 3c), there is a temperature increment related to the adsorption of carbon dioxide (around 20 K) due to the higher heat of adsorption of CO_2 comparing with adsorption heat of CH_4 (-28.5 and −11 kJ/mol, respectively). Accordingly, the temperature history of all process is dominated by adsorption–desorption of CO_2. As can be found in Fig. 3, there is an admissible agreement between the simulation results and experimental ones, which demonstrates that the developed model represents a satisfactory potential for predicting the breakthrough outcomes.

Fig. 4 represents a pseudo binary experiment of carbon dioxide and methane on the fixed bed adsorption column ((4a) partial flowrate, (4b) molar fraction and (4c) temperature history). One can observe, the simulation results with considered the DSL model can properly describes the experimental breakthrough assessments. Fig. 4a illustrates a comparison between the CO_2 and CH_4 flowrates through the adsorption and desorption experiments, which truly demonstrates the typical roll-up effect. As can be observed, the molar flowrate of light component almost is the double of the inlet molar flowrate due to the displacement with heavy component (CO_2). Accordingly, it can be considered as an experimental proof of strong competitive adsorption for displacing adsorbed methane molecules with carbon dioxide. Concerning the temperature history (Fig. 4c), as expected, during the pseudo-experiment of carbon dioxide and methane adsorption there are two peaks of temperature, unlike what happened in the previous experiment. In this particular one, the CO_2 adsorption continues in the third step. Hence, the temperature still increases due to the CO_2 energy of adsorption being higher than CH_4. Still in Fig. 4c, it can be noted that the first peak is higher than the second one. It can be explained due to during the second peak of temperature, CO_2 adsorbed amount is a little lower than the amount adsorbed in the previous step. Once again, a proper agreement among the experimental outcomes (specified by symbols) and modeling results (specified by lines) are detected in Fig. 4, providing that the considered model is reliable for designing/developing cyclic adsorption process. Taking into account the promising results of experimental and simulation outcomes, a PSA process was designed, afterwards, validated experimentally regarding the separation of carbon dioxide and methane (50 %:50 %) to biogas upgrading application. Finally, to demonstrate the appealing potential of shaped MIL-160(Al) for large scale applications, an industrial PSA scale has been designed and investigated, as well.

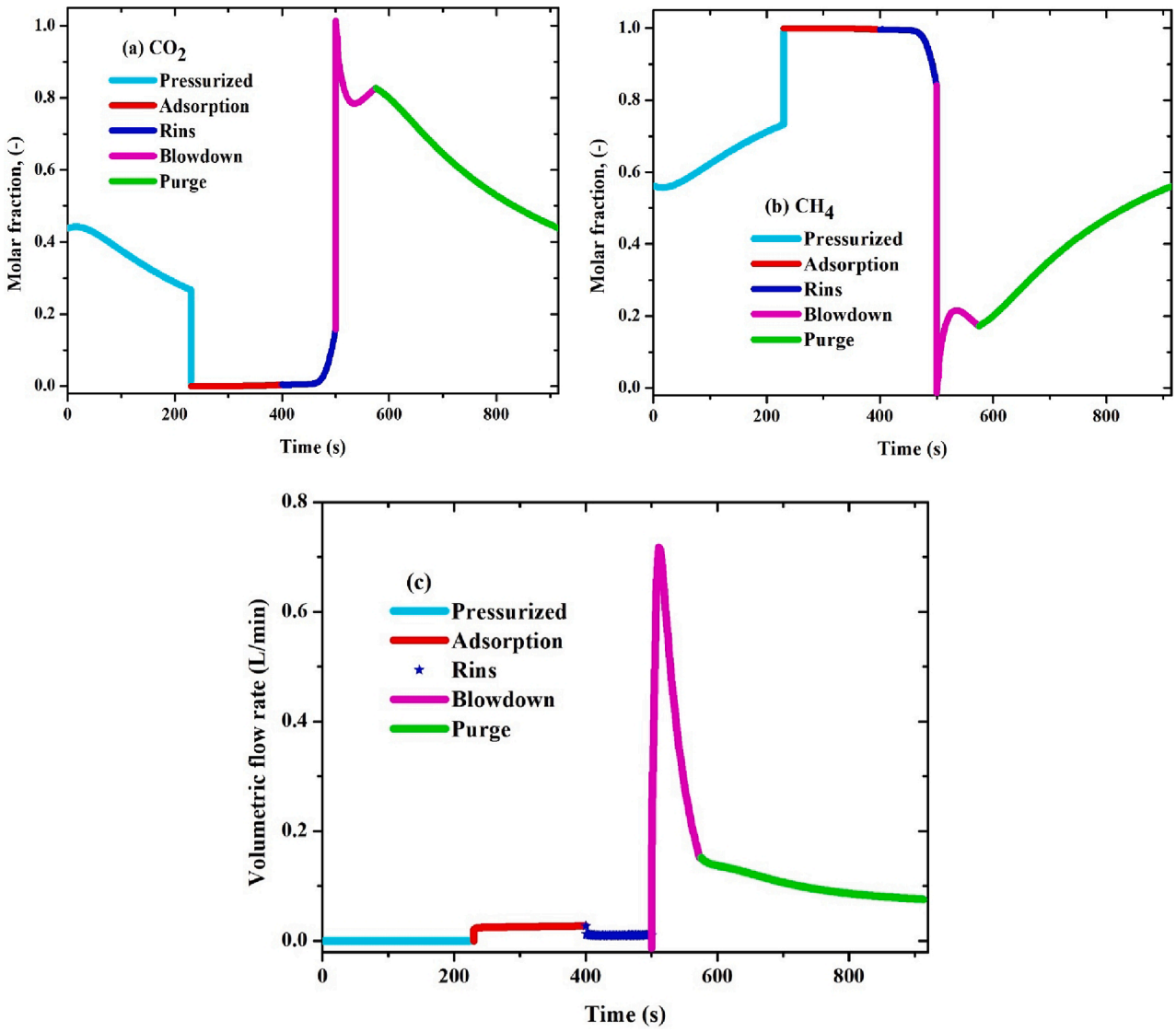

Fig. 8. The outcomes of developed industrial PSA process at the end of each step of the cyclic steady state (CSS), at 318 K and 4.0 bar. (a) carbon dioxide molar fraction (b) methane molar fraction, and (c) total volumetric flowrate.

4.2. Lab-scale cyclic adsorption experiment

Relying on the dynamic fixed-bed adsorption outcomes, a cyclic adsorption process containing five main steps including: counter-current pressurization, adsorption (feed), rinse, counter-current blowdown, and purge was designed and experimentally validated for biogas upgrading. Totally, the experimental outcomes are properly described with the designed simulation, and of course some incongruity related to the dynamic of system. The total time of cycles was around 811 s including pressurization: 51 s; feed:300 s; rinse: 350 s, blowdown: 50 s and purge: 60 s. More details related to each step are represented in Table 4.

The experimental and simulation outcomes at the end of each step of the cyclic steady state (CSS) are illustrated in Fig. 5 & 6. As shown in Fig. 5a, through the pressurization step, the column is pressurized up to 4.5 bar by the pure methane, whereas this pressure is kept in feed (adsorption) and rinse steps. In the regeneration steps (blowdown and purge), the pressure is decreased to the atmospheric pressure. However, regarding to some restrictions related to existing set-up, is not possible to achieve the vacuum pressure. As can be seen, the experimental and simulation results demonstrate a good agreement. The temperature history is also represented in Fig. 5b, which demonstrates around 20 K temperature oscillation in each cycle. Further, molar fraction of carbon dioxide and methane accompanied with the total flowrate of the represented CSS are illustrated in Fig. 6. As shown in Fig. 6a & b, the dominated tendency of methane and carbon dioxide percentage through the five steps have been properly predicted by the simulation results. Accordingly, through the pressurization step, the bed is almost saturated by countercurrent methane flow and prepared for adsorption step (as shown in Fig. 6a). During the rinse step, the fraction of CO_2 is increased for subsequent production regarding the cleaning the bed (as observed in Fig. 6a), as well as the methane is produced through this step. After the blowdown, the cycle is warped up by purge step, which through this phase, a fraction of the produced CH_4 is counter currently fed to the column at low pressure to effectively regenerate the bed and making it possible, getting high purity methane in the next cycle.

4.3. Industrial scale PSA evaluation

To evaluate the capacity of shaped MIL-160(Al) for large scale applications, in the next attempt, an industrial scale PSA was designed concerning biogas upgrading. To this end, the designed specifications were considered based on details described by [17,54]. Accordingly, the considered characterization of the current study is reported in Table 6. To achieve the highest possible purity, a PSA process with 5 different

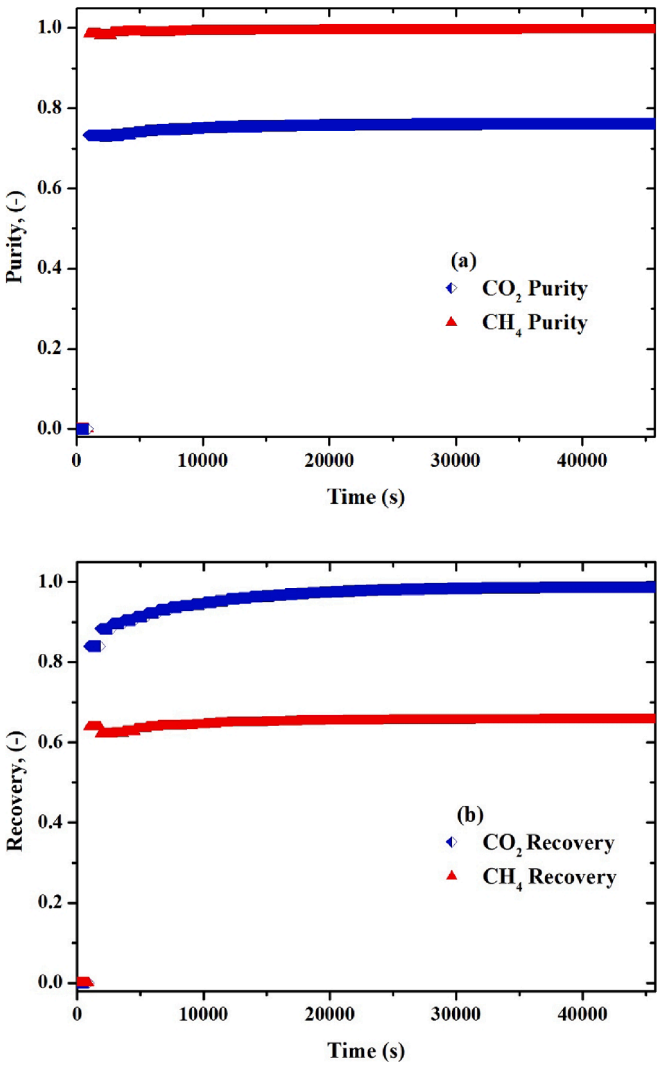

Fig. 9. (a) The purity and (b) recovery of methane and carbon dioxide on designed industrial PSA process throughout all process (50 cycles).

steps including: pressurization, feed (adsorption), rinse, blowdown, and purge was considered, which the detailed description of designed PSA is represented in Table 7. The process was assumed as a non-adiabatic, non-isotherm system, which the feed with 50 %CO_2-50 %CH_4 was fed to the column at 318 K to pass through 4 bar (in pressurization step) to 0.2 bar (in purge step). Further, the total duration of each cycle was 915 s, including pressurization step: 230 s; feed (adsorption) step: 170 s; rinse step: 100 s; blowdown step: 75 s; purge step 340 s. The simulation was developed for total number of 50 cycles, while after around 20 cycles the CSS emerged in the process.

Fig. 7 represents the pressure and temperature history at the end of each step of a CSS. The bed is firstly prepared by feeding a pure flow of CH_4 co-currently, till 4 bar, as displayed in Fig. 7a, which the methane adsorption results in temperature increment, as shown in Fig. 7b. Throughout the adsorption step, due to the carbon dioxide adsorption, a temperature peak is observed. The temperature enhancement continues during the rinse step, even more, related to pure adsorption of CO_2, while during the desorption steps (blowdown and purge), the pressure and temperature reduce, remarkably. Fig. 8, also illustrates, the carbon dioxide and methane behaviour at the end of each step of a CSS. Accordingly, the methane stream is fed to the bed during the pressurization step, which contributes to a bed almost only containing CH_4, that is ready for adsorption step (as exhibited in Fig. 8a&b). However, a rinse step (as a pure flow of CO_2) is considered to regenerate the bed and enhance the CO_2 molar fraction for next production. Accordingly, when the rinse step come to end, the bed is almost fully saturated with CO_2. Accordingly, all over the regeneration steps, the CO_2 concentration decreases and CH_4 enhances, hence, this orientation is more significant through the purge step, which in this step, a pure flow of CH_4 is counter currently fed to the column, as shown in Fig. 8a & b, until reaching the vacuum pressure at 0.2 bar, as specified in Fig. 7a, that prepares it for the next cycle. The performance of the developed process, calculated based on Eqs: 3–7, is illustrated in Fig. 9. As can be detected in Fig. 9a, in this process, the CH_4 is produced by the purity of 99.5 %, while the purity of CO_2 is around 76 %. Further, the recovery of CH_4 and CO_2 are around 66 % and 97 %, respectively. It is worth noting that the CSS cycles of designed process is represented in Appendix B (Supporting Information). As an evaluation, the potential of MIL-160(Al) for biogas upgrading has been compared with other benchmark adsorbents in Table 8. Accordingly, concerning the attractive characteristics of MIL-160(Al) including shaping in an easy way, stability, and cost [36,45,46], it represents a very competitive potential for industrial scale biogas upgrading. However, the challenge of biogas upgrading under the wet operating conditions or considering other impurities such as H_2S in the feed can be investigated as future studies.

5. Conclusions

The shaped form of the bioderived Al dicarboxylate MIL-160(Al) MOF was successfully investigated for separation of carbon dioxide and methane concerning the biogas upgrading application using a PSA process. This sample is known for water stability and being synthesized with a rational cost in a sustainable way. The fixed-bed breakthrough tests were developed as single and pseudo binary experiments at 313 K and 4.0 bar. The dynamic adsorption equilibrium outcomes were modelled using the Dual-Site Langmuir accompanied with a set of mass, energy, momentum balances as well as auxiliary relations. The breakthrough results proved the potential of considered model for predicting and developing the PSA process. Accordingly, a lab-scale PSA process with 5-steps demonstrated the well potential of MIL-160(Al) for biogas upgrading. Afterwards, a PSA process was designed in the industrial-scale considering a mixture of 40 %-60 % CO_2:CH_4 at 318 K and 4 bar. The designed PSA illustrated the purity and recovery of methane around by 99 % and 66 %, also in the case of carbon dioxide around 76 % and 97 %, respectively. The outcomes of this work indicated the superb capacity of MIL-160(Al) for biogas upgrading concerning its unparalleled specifications such as adsorption performance, synthesized cost, easy shaping, and stability comparing with other sorbents.

CRediT authorship contribution statement

Mohsen Karimi: Writing – review & editing, Writing – original draft, Validation, Software, Methodology, Investigation, Formal analysis, Conceptualization. **Rafael M. Siqueira:** Writing – review & editing, Software, Methodology, Investigation, Data curation, Conceptualization. **Alírio E. Rodrigues:** Writing – review & editing, Validation, Supervision, Project administration, Funding acquisition. **Farid Nouar:** Writing – review & editing, Validation, Resources. **José A.C. Silva:** Writing – review & editing, Supervision, Resources, Project administration, Funding acquisition. **Christian Serre:** Writing – review & editing, Validation, Supervision, Resources, Project administration. **Alexandre Ferreira:** Writing – review & editing, Validation, Supervision, Project administration, Funding acquisition, Data curation.

Declaration of competing interest

The authors declare that they have no known competing financial interests or personal relationships that could have appeared to influence the work reported in this paper.

Table 8
A comparison between the potential of some of the benchmark adsorbents for biogas upgrading using PSA process.

Adsorbent	*Process description*	*Feed specification*	*Operating conditions*		*PSA Performance*		*Cycle time (s)*	*Productivity* (mol/kg.h)	*Description*	*Ref*
			Temperature (K)	*Pressure range (bar)*	*CH_4 purity (%)*	*CH_4 recovery (%)*				
Zeolite 13X	2-bed, 6-step	67:33 % CH_4-CO_2	323	1–4.0	99.84	83.16	850	5.43	Simulation and experiments in lab scale	[55]
Zeolite 13X	2-bed, 6-step	67:33 % CH_4-CO_2	323	0.3–8.0	98.60	77.50	NA	NA	Simulation and experiments in bench scale	[56]
Zeolite 13X	2-bed, 8-step	64:35:0.01 % CH_4-CO_2-H_2S	298	0.3–4.0	95.47	91.27	850	NA	Simulation and experiments in lab scale	[57]
Zeolite NaUSY	2-bed, 4-step	58:42 % CH_4-CO_2	303	0.1–1.5	99.28	85.94	336	15.58	Simulation and experiments in bench scale	[58]
Zeolite 5 A	4-bed, 6-step	60:40 % CH_4-CO_2	NA	0.2–6.0	98.90	83.90	760	NA	Simulation in bench scale	[59]
Zeolite NaUSY	3-bed, 9-step	50:50 % CH_4-CO_2	313	0.1–2.0	99.40	96.90	NA	NA	Simulation and experiments in lab scale	[60]
Silica gel	4-bed, 9-step	55:45 % CH_4-CO_2	NA	0.1–4.0	99.56	56.95	NA	NA	Simulation and experiments in bench scale	[61]
Silica gel	2-bed, 4-step	55:45 % CH_4-CO_2	303	1–4.0	97.17	87.26	228	NA	Simulation and experiments in lab scale	[62]
CMS KP 407	2-bed, 6-step	60:40 % CH_4-CO_2	303	0.1–5.0	99.36	83.80	NA	3.46	Simulation and experiments in bench scale	[63]
CMS KP 407	3-bed, 9-step	60:40 % CH_4-CO_2	303	0.1–5.0	98.40	92.10	NA	2.56	Simulation and experiments in bench scale	[63]
CMS 3 K	2-bed, 6-step	55:45 % CH_4-CO_2	308	0.5–6.5	92.08	81.63	560	NA	Simulation in lab scale	[64]
CMS	3-bed, 6-step	55:45 % CH_4-CO_2	303	0.1–4.0	98.03	83.17	NA	NA	Simulation and experiments in lab scale	[65]
CMS-FB	4-bed, 7-step	54.9:45.1 % CH_4-CO_2	298	0.21–4.05	99.60	67.30	1200	NA	Simulation and experiments in bench scale	[66]
Spent coffee	2-bed, 4-step	68:32 % CH_4-CO_2	300	1–2.0	97.00	95.43	NA	NA	Simulation and experiments in lab scale	[67]
Pine sawdust AC	1-bed, 4-step	50:50 % CH_4-CO_2	303	1–3.0	96.5	58.5	1680	3.9	Simulation and experiments in lab scale	[68]
MIL-160 (Al)	1-bed, 5-step	60:40 % CH_4-CO_2	318	1–4.0	99.5	66.0	915	14.09	Simulation in industrial scale, validated by lab experiments	This work

Data availability

Data will be made available on request.

Acknowledgments

This work was financially supported by LA/P/0045/2020 (ALiCE), UIDB/50020/2020, and UIDP/50020/2020 (LSRE-LCM), funded by national funds through FCT/MCTES (PIDDAC). It also received financial support by national funds through FCT/MCTES (PIDDAC): CIMO, UIDB/00690/2020 (DOI: 10.54499/UIDB/00690/2020) and UIDP/00690/2020 (DOI: 10.54499/UIDP/00690/2020); and SusTEC, LA/P/0007/2020 (DOI: 10.54499/LA/P/0007/2020). Authors also acknowledge Kyung-Ho Cho and U-Hwang Lee from Korea Research Institute of Chemical Technology (KRICT), Republic of Korea, for their contributions in the shaping MIL-160(Al). M. Karimi acknowledges research grants awarded by Foundation of Science and Technology of Portugal (FCT) under SFRH/BD/140550/2018 project and University of Porto under FEUP-BioGasUpGMIL160 project.

Appendix A. Supplementary data

Supplementary data to this article can be found online at https://doi.org/10.1016/j.seppur.2024.127260.

References

[1] M. Karimi, M. Shirzad, J.A.C. Silva, A.E. Rodrigues, Biomass/Biochar carbon materials for CO2 capture and sequestration by cyclic adsorption processes: a review and prospects for future directions, J. CO_2 Utiliz. 57 (2022) 101890, https://doi.org/10.1016/J.JCOU.2022.101890.
[2] M. Karimi, J.A.C. Silva, C.N.D.P. Gonçalves, J.L. Diaz De Tuesta, A.E. Rodrigues, H. T. Gomes, CO2 capture in chemically and thermally modified activated Carbons using breakthrough measurements: Experimental and modeling study, Ind. Eng. Chem. Res. 57 (2018) 11154–11166, https://doi.org/10.1021/ACS.IECR.8B00953.
[3] M. Karimi, J.L. Diaz de Tuesta, C.N. Carmem, H.T. Gomes, A.E. Rodrigues, J.A. C. Silva, Compost from municipal solid wastes as a source of Biochar for CO2 capture, Chem. Eng. Technol. 43 (2020) 1336–1349, https://doi.org/10.1002/CEAT.201900108.
[4] J.G. Vitillo, M.D. Eisaman, E.S.P. Aradóttir, F. Passarini, T. Wang, S.W. Sheehan, The role of carbon capture, utilization, and storage for economic pathways that limit global warming to below 1.5°C, Iscience 25 (2022) 104237, https://doi.org/10.1016/J.ISCI.2022.104237.
[5] M. Karimi, M.R. Rahimpour, D. Iranshahi, Enhanced BTX production in refineries with sulfur dioxide oxidation by thermal integrated model, Chem. Eng. Technol. 41 (2018) 1746–1758, https://doi.org/10.1002/CEAT.201700289.
[6] H. Yang, Z. Xu, M. Fan, R. Gupta, R.B. Slimane, A.E. Bland, I. Wright, Progress in carbon dioxide separation and capture: a review, J. Environ. Sci. 20 (2008) 14–27, https://doi.org/10.1016/S1001-0742(08)60002-9.
[7] A. Naquash, M.A. Qyyum, J. Haider, A. Bokhari, H. Lim, M. Lee, State-of-the-art assessment of cryogenic technologies for biogas upgrading: energy, economic, and environmental perspectives, Renew. Sustain. Energy Rev. 154 (2022) 111826, https://doi.org/10.1016/J.RSER.2021.111826.
[8] A. Henrique, M. Karimi, J.A.C. Silva, A.E. Rodrigues, Analyses of adsorption behavior of CO2, CH4, and N2 on different types of BETA zeolites, Chem. Eng. Technol. 42 (2019) 327–342, https://doi.org/10.1002/CEAT.201800386.
[9] M. Shirzad, M. Karimi, J.A.C. Silva, A.E. Rodrigues, Moving bed reactors: challenges and Progress of Experimental and theoretical studies in a century of

Research, Ind. Eng. Chem. Res. 58 (2019) 9179–9198, https://doi.org/10.1021/ACS.IECR.9B01136.
[10] M. Shirzad, M. Karimi, A.E. Rodrigues, J.A.C. Silva, Biochar in Carbon sequestration, Materials Horizons: from Nature to Nanomaterials Part F 1442 (2023) 73–105, https://doi.org/10.1007/978-981-99-5239-7_4/TABLES/5.
[11] M. Karimi, A. Hosin Alibak, S. Mehdi Seyed Alizadeh, M. Sharif, B. Vaferi, Intelligent modeling for considering the effect of bio-source type and appearance shape on the biomass heat capacity, Measurement (2021) 110529, https://doi.org/10.1016/J.MEASUREMENT.2021.110529.
[12] N. Scarlat, J.F. Dallemand, F. Fahl, Biogas: developments and perspectives in Europe, renew, Energy 129 (2018) 457–472, https://doi.org/10.1016/J.RENENE.2018.03.006.
[13] E. Ryckebosch, M. Drouillon, H. Vervaeren, Techniques for transformation of biogas to biomethane, Biomass Bioenergy 35 (2011) 1633–1645, https://doi.org/10.1016/J.BIOMBIOE.2011.02.033.
[14] E. Shahhoseini, M. Arefifard, M. Karimi, Biochar for climate change mitigation, Materials Horizons: from Nature to Nanomaterials Part F 1442 (2023) 123–143, https://doi.org/10.1007/978-981-99-5239-7_6/FIGURES/9.
[15] J.A. Medrano, M.A. Llosa-Tanco, V. Cechetto, D.A. Pacheco-Tanaka, F. Gallucci, Upgrading biogas with novel composite carbon molecular sieve (CCMS) membranes: Experimental and techno-economic assessment, Chem. Eng. J. 394 (2020) 124957, https://doi.org/10.1016/J.CEJ.2020.124957.
[16] B. Verougstraete, M. Schoukens, B. Sutens, N. Vanden Haute, Y. De Vos, M. Rombouts, J.F.M. Denayer, Electrical swing adsorption on 3D-printed activated carbon monoliths for CO2 capture from biogas, Sep. Purif. Technol. 299 (2022) 121660, https://doi.org/10.1016/J.SEPPUR.2022.121660.
[17] A.F.P. Ferreira, A.M. Ribeiro, S. Kulaç, A.E. Rodrigues, Methane purification by adsorptive processes on MIL-53(Al), Chem. Eng. Sci. 124 (2015) 79–95, https://doi.org/10.1016/J.CES.2014.06.014.
[18] L.A.M. Rocha, K.A. Andreassen, C.A. Grande, Separation of CO2/CH4 using carbon molecular sieve (CMS) at low and high pressure, Chem. Eng. Sci. 164 (2017) 148–157, https://doi.org/10.1016/J.CES.2017.01.071.
[19] D. Papurello, S. Silvestri, A. Lanzini, Biogas cleaning: Trace compounds removal with model validation, Sep. Purif. Technol. 210 (2019) 80–92, https://doi.org/10.1016/J.SEPPUR.2018.07.081.
[20] M. Karimi, A.E. Rodrigues, J.A.C. Silva, Biomass as a Source of Adsorbents for CO_2 Capture, in: Advances in Bioenergy and Microfluidic Applications, Elsevier, Amsterdam, 2021: pp. 255–274.
[21] S.F. Ahmed, M. Mofijur, K. Tarannum, A.T. Chowdhury, N. Rafa, S. Nuzhat, P.S. Kumar, D.V.N. Vo, E. Lichtfouse, T.M.I. Mahlia, Biogas upgrading, economy and utilization: a review, Environ. Chem. Lett. 19(6) (2021) 4137–4164. doi: 10.1007/S10311-021-01292-X.
[22] N. Álvarez-Gutiérrez, S. García, M.V. Gil, F. Rubiera, C. Pevida, Towards bio-upgrading of biogas: biomass waste-based adsorbents, Energy Procedia 63 (2014) 6527–6533, https://doi.org/10.1016/J.EGYPRO.2014.11.688.
[23] M. Karimi, M. Shirzad, J.A.C. Silva, A.E. Rodrigues, Carbon dioxide separation and capture by adsorption: a review, Environ. Chem. Lett. 2023 (1) (2023) 1–44, https://doi.org/10.1007/S10311-023-01589-Z.
[24] M. Žák, H. Bendová, K. Friess, J.E. Bara, P. Izák, Single-step purification of raw biogas to biomethane quality by hollow fiber membranes without any pretreatment – an innovation in biogas upgrading, Sep. Purif. Technol. 203 (2018) 36–40, https://doi.org/10.1016/J.SEPPUR.2018.04.024.
[25] B. Aghel, A. Gouran, S. Behaien, B. Vaferi, Experimental and modeling analyzing the biogas upgrading in the microchannel: Carbon dioxide capture by seawater enriched with low-cost waste materials, Environ. Technol. Innov. 27 (2022) 102770, https://doi.org/10.1016/J.ETI.2022.102770.
[26] C.W. Skarstrom, O.-O.I. Attorney, Method and apparatus for fractionating gaseous mixtures by adsorption, (1958).
[27] B. Yuan, X. Wu, Y. Chen, J. Huang, H. Luo, S. Deng, Adsorption of CO2, CH4, and N2 on ordered mesoporous carbon: approach for greenhouse gases capture and biogas upgrading, Environ. Sci. Tech. 47 (2013) 5474–5480, https://doi.org/10.1021/ES4000643/SUPPL_FILE/ES4000643_SI_002.PDF.
[28] Z. Xiang, X. Peng, X. Cheng, X. Li, D. Cao, CNT@Cu3(BTC)2 and metal-organic frameworks for Separation of CO2/CH4 mixture, J. Phys. Chem. C 115 (2011) 19864–19871, https://doi.org/10.1021/jp206959k.
[29] R.L.S. Canevesi, K.A. Andreassen, E.A. da Silva, C.E. Borba, C.A. Grande, Pressure swing adsorption for biogas upgrading with Carbon Molecular sieve, Ind. Eng. Chem. Res. 57 (2018) 8057–8067, https://doi.org/10.1021/acs.iecr.8b00996.
[30] R. Canevesi, C.A. Grande, Biogas upgrading by pressure swing adsorption using zeolite 4A. Effect of purge on process performance, Sep. Purif. Technol. 309 (2023) 123015, https://doi.org/10.1016/J.SEPPUR.2022.123015.
[31] M. Karimi, L.F.A.S. Zafanelli, J.P.P. Almeida, G.R. Ströher, A.E. Rodrigues, J.A. C. Silva, Novel insights into activated Carbon derived from municipal solid waste for CO2Uptake: synthesis, adsorption isotherms and scale-up, J. Environ. Chem. Eng. 8 (2020), https://doi.org/10.1016/J.JECE.2020.104069.
[32] I. Durán, N. Álvarez-Gutiérrez, F. Rubiera, C. Pevida, Biogas purification by means of adsorption on pine sawdust-based activated carbon: impact of water vapor, Chem. Eng. J. 353 (2018) 197–207, https://doi.org/10.1016/J.CEJ.2018.07.100.
[33] L. Joss, M. Gazzani, M. Mazzotti, Rational design of temperature swing adsorption cycles for post-combustion CO2 capture, Chem. Eng. Sci. 158 (2017) 381–394, https://doi.org/10.1016/J.CES.2016.10.013.
[34] L.F.A.S. Zafanelli, A. Henrique, M. Karimi, A.E. Rodrigues, J.A.C. Silva, Single- a nd multicomponent fixed bed adsorption of CO2, CH4, and N2in binder-free beads of 4A zeolite, Ind. Eng. Chem. Res. 59 (2020) 13724–13734, https://doi.org/10.1021/ACS.IECR.0C01911/SUPPL_FILE/IE0C01911_SI_001.PDF.
[35] M. Karimi, A.E. Rodrigues, J.A.C. Silva, Designing a simple volumetric apparatus for measuring gas adsorption equilibria and kinetics of sorption. application and validation for CO2, CH4 and N2 adsorption in binder-free beads of 4A zeolite, Chem. Eng. J. 425 (2021) 130538, https://doi.org/10.1016/J.CEJ.2021.130538.
[36] M.I. Severino, E. Gkaniatsou, F. Nouar, M.L. Pinto, C. Serre, MOFs industrialization: a complete assessment of production costs, Faraday Discuss. 231 (2021) 326–341, https://doi.org/10.1039/D1FD00018G.
[37] S. Keskin, T.M. van Heest, D.S. Sholl, Can metal-organic framework materials play a useful role in Large-scale Carbon dioxide Separations? ChemSusChem 3 (2010) 879–891, https://doi.org/10.1002/CSSC.201000114.
[38] M. Ding, R.W. Flaig, H.L. Jiang, O.M. Yaghi, Carbon capture and conversion using metal–organic frameworks and MOF-based materials, Chem. Soc. Rev. 48 (2019) 2783–2828, https://doi.org/10.1039/C8CS00829A.
[39] S. Dai, A. Tissot, C. Serre, Recent progresses in metal-organic frameworks based Core–shell composites, Adv. Energy Mater. 12 (2022) 2100061, https://doi.org/10.1002/AENM.202100061.
[40] M. Karimi, A. Ferreira, A.E. Rodrigues, F. Nouar, C. Serre, J.A.C. Silva, MIL-160(Al) as a candidate for biogas upgrading and CO 2 capture by adsorption processes, Ind. Eng. Chem. Res. (2023), https://doi.org/10.1021/ACS.IECR.2C04150/SUPPL_FILE/IE2C04150_SI_001.PDF.
[41] G. Mouchaham, F.S. Cui, F. Nouar, V. Pimenta, J.S. Chang, C. Serre, Metal-organic frameworks and water: 'from old enemies to friends'? Trends Chem 2 (2020) 990–1003, https://doi.org/10.1016/j.trechm.2020.09.004.
[42] D. Chakraborty, A. Yurdusen, G. Mouchaham, F. Nouar, C. Serre, Large-scale production of metal-organic frameworks, Adv. Funct. Mater. (2023) 2309089, https://doi.org/10.1002/ADFM.202309089.
[43] A.A. Abd, M.R. Othman, I.K. Shamsudin, Z. Helwani, I. Idris, Biogas upgrading to natural gas pipeline quality using pressure swing adsorption for CO2 separation over UiO-66: Experimental and dynamic modelling assessment, Chem. Eng. J. 453 (2023) 139774, https://doi.org/10.1016/J.CEJ.2022.139774.
[44] M.P. Silva, A.M. Ribeiro, C.G. Silva, K. Ho Cho, U.H. Lee, J.L. Faria, J.M. Loureiro, J.S. Chang, A.E. Rodrigues, A. Ferreira, Atmospheric water harvesting on MIL-100 (Fe) upon a cyclic adsorption process, Sep. Purif. Technol. 290 (2022) 120803, https://doi.org/10.1016/J.SEPPUR.2022.120803.
[45] A. Cadiau, J.S. Lee, D. Borges, P. Fabry, T. Devic, M.T. Wharmby, C. Martineau, D. Foucher, F. Taulelle, C.-H. Jun, Y.K. Hwang, N. Stock, M.F. De Lange, F. Kapteijn, J. Gascon, G. Maurin, J.-S. Chang, C. Serre, A. Cadiau, P. Fabry, T. Devic, C. Martineau, D. Foucher, F. Taulelle, C. Serre, J.S. Lee, Y.K. Hwang, J.-S. Chang, C.-H. Jun, D. Damasceno-Borges, G. Maurin, M.F. De Lange, F. Kapteijn, J. Gascon, Design of hydrophilic metal organic framework water adsorbents for heat reallocation, Adv. Mater. 27 (2015) 4775–4780, https://doi.org/10.1002/ADMA.201502418.
[46] A. Permyakova, O. Skrylnyk, E. Courbon, M. Affram, S. Wang, U.H. Lee, A. H. Valekar, F. Nouar, G. Mouchaham, T. Devic, G. de Weireld, J.S. Chang, N. Steunou, M. Frère, C. Serre, Synthesis optimization, shaping, and heat reallocation evaluation of the hydrophilic metal-organic framework MIL-160(Al), ChemSusChem 10 (2017) 1419–1426, https://doi.org/10.1002/CSSC.201700164.
[47] D. Damasceno Borges, G. Maurin, D.S. Galvaõ, Design of Porous Metal-Organic Frameworks for Adsorption Driven Thermal Batteries, MRS Adv. 9(2) (2017) 519–524. doi: 10.1557/ADV.2017.181.
[48] P.F. Brântuas, A. Henrique, M. Wahiduzzaman, A. Von Wedelstedt, T. Maity, A. E. Rodrigues, F. Nouar, U.-H. Lee, K.-H. Cho, G. Maurin, J.A.C. Silva, C. Serre, P. F. Brântuas, A. Henrique, T. Maity, J.A.C. Silva, A.E. Rodrigues, Separation of branched alkanes feeds by a synergistic action of zeolite and metal-organic framework, Adv. Sci. 9 (2022) 2201494, https://doi.org/10.1002/ADVS.202201494.
[49] M. Karimi, Process development for Carbon dioxide capture using novel adsorbents: applications for clean energy and environmental protection, University of Porto, 2023.
[50] D.D. Do, Adsorption Analysis: Equilibria and Kinetics (With CD Containing Computer Matlab Programs), 1st ed., Imperial College Press, London, 1998. doi: 10.1142/P111.
[51] R. Seabra, A.M. Ribeiro, K. Gleichmann, A.F.P. Ferreira, A.E. Rodrigues, Adsorption equilibrium and kinetics of carbon dioxide, methane and nitrogen on binderless zeolite 4A adsorbents, Microporous Mesoporous Mater. 277 (2019) 105–114, https://doi.org/10.1016/J.MICROMESO.2018.10.024.
[52] D.M. Ruthven, Principles of adsorption and adsorption processes, 1st ed., Wiley, New York, 1984.
[53] R. Rota, P.C. Wankat, Intensification of pressure swing adsorption processes, AIChE J 36 (1990) 1299–1312, https://doi.org/10.1002/AIC.690360903.
[54] A.M. Ribeiro, J.C. Santos, A.E. Rodrigues, PSA design for stoichiometric adjustment of bio-syngas for methanol production and co-capture of carbon dioxide, Chem. Eng. J. 163 (2010) 355–363, https://doi.org/10.1016/J.CEJ.2010.08.015.
[55] M.P.S. Santos, C.A. Grande, A.E. Rodrigues, Pressure swing adsorption for biogas upgrading. Effect of recycling streams in pressure swing adsorption design, Ind. Eng. Chem. Res. 50 (2010) 974–985, https://doi.org/10.1021/IE100757U.
[56] B. Wu, X. Zhang, Y. Xu, D. Bao, S. Zhang, Assessment of the energy consumption of the biogas upgrading process with pressure swing adsorption using novel adsorbents, J. Clean. Prod. 101 (2015) 251–261, https://doi.org/10.1016/J.JCLEPRO.2015.03.082.
[57] Y.F. Chen, P.W. Lin, W.H. Chen, F.Y. Yen, H.S. Yang, C.T. Chou, Biogas Upgrading by Pressure Swing Adsorption with Design of Experiments, Processes 2021, Vol. 9, Page 1325 9 (2021) 1325. doi: 10.3390/PR9081325.
[58] A. Arya, S. Divekar, R. Rawat, P. Gupta, M.O. Garg, S. Dasgupta, A. Nanoti, R. Singh, P. Xiao, P.A. Webley, Upgrading biogas at low pressure by vacuum swing

adsorption, Ind. Eng. Chem. Res. 54 (2015) 404–413, https://doi.org/10.1021/IE503243F/SUPPL_FILE/IE503243F_SI_001.PDF.
[59] R. Augelletti, M. Conti, M.C. Annesini, Pressure swing adsorption for biogas upgrading. A new process configuration for the separation of biomethane and carbon dioxide, J. Clean. Prod. 140 (2017) 1390–1398, https://doi.org/10.1016/J.JCLEPRO.2016.10.013.
[60] Y. Jiang, J. Ling, P. Xiao, Y. He, Q. Zhao, Z. Chu, Y. Liu, Z. Li, P.A. Webley, Simultaneous biogas purification and CO2 capture by vacuum swing adsorption using zeolite NaUSY, Chem. Eng. J. 334 (2018) 2593–2602, https://doi.org/10.1016/J.CEJ.2017.11.090.
[61] Y. Shen, W. Shi, D. Zhang, P. Na, B. Fu, The removal and capture of CO2 from biogas by vacuum pressure swing process using silica gel, J. CO2 Util. 27 (2018) 259–271, https://doi.org/10.1016/J.JCOU.2018.08.001.
[62] A. Ali Abd, M. Roslee Othman, Biogas upgrading to fuel grade methane using pressure swing adsorption: Parametric sensitivity analysis on an industrial scale, Fuel 308 (2022) 121986, https://doi.org/10.1016/J.FUEL.2021.121986.
[63] R.L.S. Canevesi, K.A. Andreassen, E.A. Silva, C.E. Borba, C.A. Grande, Evaluation of simplified pressure swing adsorption cycles for bio-methane production, Adsorption 25 (2019) 783–793, https://doi.org/10.1007/S10450-019-00049-X/METRICS.
[64] B. Kottititum, T. Srinophakun, N. Phongsai, Q.T. Phung, Optimization of a Six-Step Pressure Swing Adsorption Process for Biogas Separation on a Commercial Scale, Appl. Sci. 10 (2020) 4692. doi: 10.3390/APP10144692.
[65] Y. Shen, Z.Y. Niu, R.Y. Zhang, D. Zhang, Vacuum pressure swing adsorption process with carbon molecular sieve for CO2 separation from biogas, J. CO2 Util. 54 (2021) 101764, https://doi.org/10.1016/J.JCOU.2021.101764.
[66] Y.J. Kim, Y.S. Nam, Y.T. Kang, Study on a numerical model and PSA (pressure swing adsorption) process experiment for CH4/CO2 separation from biogas, Energy 91 (2015) 732–741, https://doi.org/10.1016/J.ENERGY.2015.08.086.
[67] A.A. Abd, M.R. Othman, H.J.K. Shabbani, Z. Helwani, Biomethane upgrading to transportation fuel quality using spent coffee for carbon dioxide capture in pressure swing adsorption, J. Environ. Chem. Eng. 10 (2022) 107169, https://doi.org/10.1016/J.JECE.2022.107169.
[68] I. Durán, F. Rubiera, C. Pevida, Modeling a biogas Upgrading PSA unit with a sustainable activated carbon derived from pine sawdust. Sensitivity analysis on the adsorption of CO2 and CH4 mixtures, Chemical Engineering Journal 428 (2022) 132564, https://doi.org/10.1016/J.CEJ.2021.132564.